In vitro anti-bacterial and time kill evaluation of binuclear tricyclohexylphosphanesilver(I) dithiocarbamates, {Cy$_3$PAg(S$_2$CNRR′)}$_2$

Yi Jiun Tan[a,b], Yee Seng Tan[a], Chien Ing Yeo[a], Jactty Chew[b,*], Edward R.T. Tiekink[a,*]

[a] Research Centre for Crystalline Materials, School of Science and Technology, Sunway University, No. 5 Jalan Universiti, 47500 Bandar Sunway, Selangor Darul Ehsan, Malaysia
[b] Department of Biological Sciences, School of Science and Technology, Sunway University, No. 5 Jalan Universiti, 47500 Bandar Sunway, Selangor Darul Ehsan, Malaysia

ABSTRACT

Four binuclear phosphanesilver(I) dithiocarbamates, {cyclohexyl$_3$PAg(S$_2$CNRR′)}$_2$ for R = R′ = Et (**1**), CH$_2$CH$_2$ (**2**), CH$_2$CH$_2$OH (**3**) and R = Me, R′ = CH$_2$CH$_2$OH (**4**) have been synthesised and characterised by spectroscopy and crystallography, and feature tri-connective, μ$_2$-bridging dithiocarbamate ligands and distorted tetrahedral geometries based on PS$_3$ donor sets. The compounds were evaluated for anti-bacterial activity against a total of 12 clinically important pathogens. Based on minimum inhibitory concentration (MIC) and cell viability tests (human embryonic kidney cells, HEK 293), **1–4** are specifically active against Gram-positive bacteria while demonstrating low toxicity; **3** and **4** are active against methicillin resistant *S. aureus* (MRSA). Across the series, **4** was most effective and was more active than the standard anti-biotic chloramphenicol. Time kill assays reveal **1–4** to exhibit both time- and concentration-dependent pharmacokinetics against susceptible bacteria. Compound **4** demonstrates rapid (within 2 h) bactericidal activity at 1 and 2 × MIC to reach a maximum decrease of 5.2 log$_{10}$ CFU/mL against *S. aureus* (MRSA).

1. Introduction

The inexorable emergence of anti-biotic resistant bacteria to multiple anti-bacterial agents is now recognised as a significant global health threat worldwide as there are fewer or even no effective anti-biotic treatments available for these infectious pathogens [1]. The problem arises in part due to selective stress exerted on bacteria that is driven by the use and misuse of anti-bacterial agents in food producing animals and patients. This pressure has forced the quickly replicating bacteria to develop resistance mechanisms [2,3]. This worrying situation highlights the urgent need to develop novel and selective anti-bacterial drugs. The real challenge remains to develop new anti-bacterial agents with new mechanisms of action that can overcome acquired resistance without contributing to resistance development [4].

Historically, metal-based drugs have been used as drugs to treat a variety of diseases, i.e. platinum compounds, e.g. cisplatin, carboplatin and oxaliplatin, are the most widely used cancer therapeutic agents, and gold compounds, e.g. myocrisin and auranofin, are used for the treatment of rheumatoid arthritis [5]. Notably, silver and its compounds [6,7] and silver-based nanoparticles [8] have long been known to possess strong inhibitory and bactericidal effects as well as a broad spectrum of anti-microbial activities for bacteria, fungi and viruses, and

continue to attract significant attention [9–12]. Silver generally exhibits higher toxicity to microorganisms with lower toxicity to mammalian cells compared with other metals [13].

Recent studies have highlighted metal dithiocarbamate derivatives, M^y(S$_2$CNRR′)$_y$, as potential metal-based drugs to combat bacterial infection [14]. Thus, over the years, various transition metal complexes [15–17] and main group element dithiocarbamate compounds [18–21] have been investigated in this context and interest continues with a focus of recent research being upon coinage metal dithiocarbamates, i.e. of copper(I) and silver(I) [22] and of gold(I) [23,24]. In the latter studies, emphasis has moved away from R, R′ = alkyl compounds to include hydroxyethyl substituents owing to the possibility of enhanced hydrophilicity of the resultant compounds. Noteworthy results from these previous biological assays include the observation that the anti-bacterial activity of a series phosphanegold(I) dithiocarbamates, R$_3$PAu [S$_2$CN(iPr)CH$_2$CH$_2$OH] for R = Et, cyclohexyl (Cy) and Ph, were found to be dependent on the nature of the phosphane-bound substituent. While the R = Cy and Ph derivatives exhibited specific activity against Gram-positive bacteria, the R = Et compound showed broad range activity against both Gram-positive and Gram-negative bacteria [23]. Also, based on time kill studies the R = Cy and Ph compounds were bactericidal whereas the R = Et compound was bactericidal and

1: R = R′ = Et

2: R = R′ = CH_2CH_2

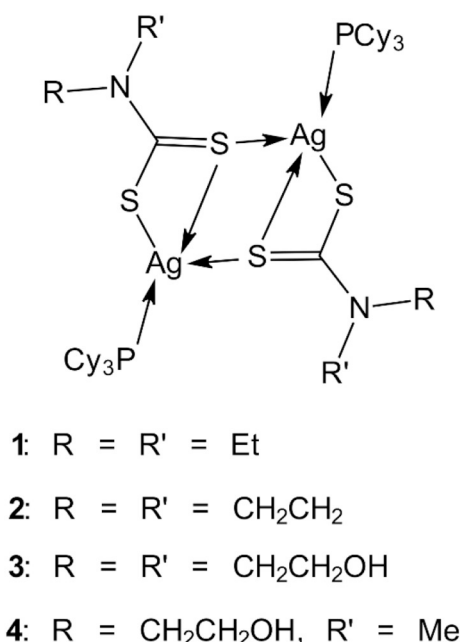**3**: R = R′ = CH_2CH_2OH

4: R = CH_2CH_2OH, R′ = Me

Fig. 1. Chemical structures of **1–4**.

bacteriostatic depending on the specific bacterial strain investigated [23]. In a latter study, a series of bis(triphenylphosphane)-copper (I) and -silver(I) dithiocarbamates were investigated as new anti-bacterial agents and revealed activities dependent upon both phosphane- and dithiocarbamate-bound substituents [22].

Reflecting the interesting results obtained for the ternary phosphane-copper (I) and silver(I) dithiocarbamate compounds in tackling pathogens and in recognition of the potential of silver dithiocarbamates as effective anti-bacterial agents, the preceding studies were extended to the four compounds shown in Fig. 1, i.e. containing tricyclohexylphosphane co-ligands. Herein, a study was conducted to determine the efficacy of **1–4** as potential anti-bacterial agents against a range of Gram-positive and Gram-negative bacteria using disc diffusion, MIC and MBC assays. To further determine the preliminary pharmacokinetics of these complexes, time kill assays were employed to assess whether the treated bacteria were bactericidal or bacteriostatic. The cytotoxicity effects of **1–4** were evaluated through a MTT (3-[4,5-dimethylthiazol-2-yl]-2,5-diphenyl tetrazolium bromide) assay on normal cells, i.e. HEK 293 human embryonic kidney epithelial cells.

2. Experimental

2.1. Materials

All chemicals and solvents were used as received. Reactions were carried out under ambient conditions. The sodium diethyldithiocarbamate trihydrate (BDH Chemicals) and ammonium pyrrolidinedithiocarbamate (Sigma-Aldrich), tricyclohexylphosphane (Cy$_3$P; Sigma-Aldrich) and AgNO$_3$ (Systerm) were obtained from commercial sources. The hydroxyethyl dithiocarbamate ligands, $^-$S$_2$CN(R)CH$_2$CH$_2$OH for R = CH$_2$CH$_2$OH and Me, as K$^+$ or NH$_4^+$ salts, were prepared as per an earlier study [25].

2.2. Instrumentation

Melting points were determined on an Automatic Melting Apparatus MP450 (Biobase, China). Elemental analyses were performed on a Leco TruSpec Micro CHN Elemental Analyser. IR spectra were obtained on a Vertex 70v FTIR Spectrometer (Bruker, Germany); abbreviations: s = strong; m = medium. ^{1}H, ^{13}C$\{^1$H$\}$ and ^{31}P$\{^1$H$\}$ NMR spectra were

recorded in CDCl$_3$ solution at 25 °C on a Bruker Ascend 400 MHz NMR spectrometer with chemical shifts relative to tetramethylsilane (internal; ^{1}H and ^{13}C$\{^1$H$\}$) and triphenylphosphate (external; ^{31}P$\{^1$H$\}$) reference; abbreviations for NMR assignments: s = singlet; d = doublet; t = triplet; q = quartet; sept = septet; m = multiplet; br = broad.

2.3. Synthesis and characterisation

2.3.1. Bis{tricyclohexylphosphanesilver(I)   N,N-diethyldithiocarbamate} (1)

Cy$_3$P (1 mmol; 0.280 g) dissolved in acetonitrile (10 mL) was added to an acetonitrile solution (10 mL) of AgNO$_3$ (1 mmol; 0.170 g) at room temperature. Then, Na[S$_2$CNEt$_2$]·3H$_2$O (1 mmol; 0.225 g) dissolved in ethanol (10 mL) was added followed by stirring for 4 h. The resulting mixture was filtered and evaporated to yield a yellow solid. The solid was recrystallized from a dichloromethane and methanol solution (4 mL; 1/1 v/v) via slow evaporation, yielding yellow crystals. Yield: 65%. M.p.: 197.7 °C. Anal. calc. for C$_{23}$H$_{43}$AgNPS$_2$: C, 51.48; H, 8.08; N, 2.61. Found: C, 51.55; H, 8.43; N, 2.65. IR (cm^{-1}): 1473 (m) ν(C−N); 1073 (m), 991 (m) ν(C−S). ^{1}H NMR: δ 3.98 (q, 4H, CH$_2$, $J_{H\text{-}H}$ = 6.96 Hz), 1.32 (t, 6H, CH$_3$, $J_{H\text{-}H}$ = 7.04 Hz), 1.89–1.20 (m, br, 33H, Cy$_3$P) ppm. ^{13}C$\{^1$H$\}$ NMR: δ 209.2 (C$_q$), 49.2 (CH$_2$), 31.9 (d, α-C$_6$H$_{11}$, $J_{C\text{-}P}$ = 14.57 Hz), 31.1 (d, β-C$_6$H$_{11}$, $J_{C\text{-}P}$ = 4.54 Hz), 27.3 (d, γ-PC$_6$H$_{11}$, $J_{C\text{-}P}$ = 11.64 Hz), 26.0 (d, δ-C$_6$H$_{11}$, $J_{C\text{-}P}$ = 0.84 Hz), 12.2 (CH$_3$) ppm. ^{31}P$\{^1$H$\}$ NMR: δ 40.0 (d, $J_{^{107}Ag\text{-}P}$ = 552.15, $J_{^{109}Ag\text{-}P}$ = 625.00 Hz) ppm.

2.3.2. Bis{tricyclohexylphosphanesilver(I) N,N-pyrrolidinedithiocarbamate} (2)

Compound **2** was prepared as for **1** but using NH$_4$[S$_2$CN(CH$_2$CH$_2$)$_2$] (1 mmol; 0.164 g) as the dithiocarbamate ligand. Yield: 41%. M.p.: 199.9 °C. Anal. calc. for C$_{23}$H$_{41}$AgNPS$_2$: C, 51.68; H, 7.73; N, 2.62. Found: C, 51.51; H, 7.77; N, 2.67. IR (cm^{-1}): 1423 (s) ν(C−N); 1032 (m), 996 (m) ν(C−S). ^{1}H NMR: δ 3.82 (t, 4H, NCH$_2$, $J_{H\text{-}H}$ = 6.44 Hz), 2.00 (t, 4H, CH$_2$, $J_{H\text{-}H}$ = 6.54 Hz), 1.92–1.17 (m, br, 33H, Cy$_3$P) ppm. ^{13}C$\{^1$H$\}$ NMR: δ 205.7 (C$_q$), 49.2 (NCH$_2$), 31.9 (d, α-C$_6$H$_{11}$, $J_{C\text{-}P}$ = 14.46 Hz), 31.1 (d, β-PC$_6$H$_{11}$, $J_{C\text{-}P}$ = 4.39 Hz), 27.3 (d, γ-C$_6$H$_{11}$, $J_{C\text{-}P}$ = 11.31 Hz), 26.6 (CH$_2$), 26.0 (δ-C$_6$H$_{11}$) ppm. ^{31}P$\{^1$H$\}$ NMR: δ 40.0 (d, $J_{^{107}Ag\text{-}P}$ = 548.75, $J_{^{109}Ag\text{-}P}$ = 631.52 Hz) ppm.

2.3.3. Bis{tricyclohexylphosphanesilver(I)   N,N-dihydroxyethyldithio carbamate} (3)

The compound was prepared from the in situ reaction of AgNO$_3$, Cy$_3$P and K[S$_2$CN(CH$_2$CH$_2$OH)$_2$] in a 1:1:1 ratio. AgNO$_3$ (1 mmol; 0.170 g) was stirred with Cy$_3$P (1 mmol; 0.280 g) in acetonitrile (10 mL) at room temperature to obtain a suspension. To this K[S$_2$CN(CH$_2$CH$_2$OH)$_2$] (1 mmol; 0.219 g) in water (4 mL)/ethanol (6 mL) mixture was added followed by stirring for 2 h. Chloroform (20 mL) was added and stirring was continued for another 2 h, after which the yellow chloroform solution was separated. The organic solution was dried over MgSO$_4$, filtered and slowly evaporated to yield a bright-yellow gel. A minimum volume of hexane (2 mL) was added to this gel while stirring vigorously until precipitation occurred. The yellow precipitates were isolated through filtration. Recrystallization was performed in methanol via slow evaporation, yielding yellow block crystals. Yield: 60%. M.p.: 180.2 °C. Anal. calc. for C$_{23}$H$_{43}$AgNO$_2$PS$_2$: C, 48.59; H, 7.62; N, 2.46. Found: C, 48.71; H, 7.93; N, 2.54. IR (cm^{-1}): 1448 (s) ν(C−N); 1066 (s), 985 (s) ν(C−S). ^{1}H NMR: δ 4.24 (s, br, 4H, OCH$_2$), 4.09 (s, br, 4H, NCH$_2$), 3.26 (s, br, 2H, OH), 1.89–1.27 (m, br, 33H, Cy$_3$P) ppm. ^{13}C$\{^1$H$\}$: δ 213.4 (C$_q$), 61.2 (OCH$_2$), 59.1 (NCH$_2$), 32.0 (d, α-C$_6$H$_{11}$, $J_{C\text{-}P}$ = 14.09 Hz), 31.1 (d, β-C$_6$H$_{11}$, $J_{C\text{-}P}$ = 4.43 Hz), 27.3 (d, γ-C$_6$H$_{11}$, $J_{C\text{-}P}$ = 11.59 Hz), 26.0 (δ-C$_6$H$_{11}$) ppm. ^{31}P$\{^1$H$\}$ NMR: δ 39.4 (d, br, $J_{Ag\text{-}P}$ = 590.94 Hz) ppm.

2.3.4. Bis{tricyclohexylphosphanesilver(I) N-hydroxyethyl-N-methyldithio carbamate} (4)

AgNO$_3$ (1 mmol; 0.170 g) was stirred with Cy$_3$P (1 mmol; 0.280 g) in acetonitrile (10 mL) at room temperature to yield a suspension. Then,

$NH_4[S_2CN(Me)CH_2CH_2OH)]$ (1 mmol; 0.168 g) in water (10 mL) was added which was then stirred for 2 h. Chloroform (20 mL) was added and stirring was continued for another 2 h, after which the yellow chloroform solution was separated. The solution was filtered and evaporated to yield a yellow solid. The crystals were obtained from dichloromethane by slow evaporation. Yield: 71%. M.p.: 183.3 °C. Anal. calc. for $C_{22}H_{41}AgNOPS_2$: C, 49.07; H, 7.67; N, 2.60. Found: C, 48.93; H, 8.13; N, 2.47. IR (cm^{-1}): 1443 (m) ν(C−N); 1043 (m), 993 (m) ν(C−S). ^1H NMR: δ 4.20 (t, 2H, OCH_2, J_{H-H} = 5.20 Hz), 4.01 (t, 2H, NCH_2, J_{H-H} = 5.00 Hz), 3.56 (s, 3H, CH_3), 2.64 (s, br, 1H, OH), 1.88–1.17 (m, br, 33H, Cy_3P) ppm. $^{13}C\{^1H\}$ NMR: δ 212.1 (C_q), 61.0 (OCH_2), 59.1 (NCH_2), 44.5 (CH_3), 32.0 (d, α-C_6H_{11}, J_{C-P} = 14.26 Hz), 31.1 (d, β-PC_6H_{11}, J_{C-P} = 4.54 Hz), 27.3 (d, γ-C_6H_{11}, J_{C-P} = 11.54 Hz), 26.0 (δ-C_6H_{11}) ppm. $^{31}P\{^1H\}$ NMR: δ 39.7 (d, $J_{107Ag-P}$ = 554.91, $J_{109Ag-P}$ = 629.68 Hz) ppm.

2.4. Single crystal X-ray structure determinations

Intensity data for **1**–**4** were measured at 100 K on an Rigaku/Oxford Diffraction XtaLAB Synergy diffractometer (Dualflex, AtlasS2) using CuKα radiation (λ = 1.54178 Å). Data reduction and Gaussian absorption corrections were by standard methods [26]. The structures were solved by direct methods [27] and refined on F^2 with anisotropic displacement parameters and C-bound H atoms in the riding model approximation [28]. For **3** and **4**, the O-bound H atoms were located from Fourier difference maps but refined with O−H constrained to 0.84 ± 0.01 Å. A weighting scheme of the form w = 1/$[\sigma^2(F_o^2) + (aP)^2 + bP]$ where P = $((F_o^2 + 2F_c^2) / 3)$ was introduced in each case. In the refinement of **2**, a second position was detected for the Ag1 with the minor component, after unrestrained refinement, having a site occupancy = 0.280(14); no evidence for other disordered atoms was found. The maximum and minimum residual electron density peaks of 1.15 and 0.61 e$Å^{-3}$, respectively, were located 0.87 and 0.39 Å from the C18 and H23a atoms, respectively. In the refinement of **4**, the C11-cyclohexyl ring was disordered over two positions. Anisotropic refinement but, with the displacement ellipsoids constrained to be nearly isotropic, led to a site occupancy factor = 0.571(11) for the major component. The maximum and minimum residual electron density peaks of 1.15 and 1.32 e$Å^{-3}$, respectively, were located 0.98 and 0.75 Å from the H26c and Ag1 atoms, respectively. Crystal data and refinement details are collected in Table 1. The molecular structure diagrams showing 70% probability displacement ellipsoids were generated by ORTEP for Windows [29] and the packing diagrams with DIAMOND [30]. Additional data analysis was made with PLATON [31]. Data for **1**–**4**, in the form of Crystallographic Information Files (CIF's) have been deposited with the Cambridge Structural Database with deposition nos: 1865251–1865254.

2.5. Anti-bacterial activity studies

2.5.1. Preparation of test organisms

A total of 12 clinically important pathogens were used in this study and these were purchased from either the American Type Culture Collection (ATCC) or the Malaysian Type Culture Collection (MTCC). Five Gram-positive bacteria, i.e. *Enterococcus faecalis* (ATCC 33186), a clinical isolate of methicillin-resistant *Staphylococcus aureus* (MRSA) (MTCC 381123), *Staphylococcus epidermidis* (ATCC 700576), *Streptococcus pneumoniae* (ATCC 49619) and *Streptococcus pyogenes* (ATCC 49399), and seven Gram-negative bacteria, i.e. *Escherichia coli* (ATCC 11775), *Escherichia coli* (MTCC 710859), *Klebsiella pneumoniae* (ATCC 13883), *Klebsiella quasipneumoniae* (ATCC 700603), *Pseudomonas aeruginosa* (ATCC 10145), *Proteus mirabilis* (ATCC 25933) and *Salmonella enterica* (ATCC 14028). Fastidious bacteria, *S. pneumoniae* and *S. pyogenes*, were cultured in Mueller-Hinton Broth (MHB) (Oxoid), while all remaining bacteria were cultured in Nutrient Broth (NB) (Oxoid) and grown overnight at 37 °C prior to experiments.

2.5.2. Disc diffusion

The disc diffusion method was used to screen for anti-bacterial activity of the synthesised compounds in accordance with the Clinical and Laboratory Standards Institute (CLSI) guidelines. An inoculum suspension of each bacterial strain was prepared by adjusting the overnight bacterial culture to 0.5 McFarland turbidity standard, corresponding to approximately 10^8 colony forming units CFU/mL. The inoculum was swabbed on the surface of Mueller-Hinton agar (MHA) (Oxoid) plates using a sterile cotton swab. The test compounds were taken up in dimethylsulphoxide (DMSO; Merck) to achieve a test concentration of 2 mg/mL; **1** and **2** were suspensions. Sterile 6 mm filter paper discs were aseptically placed on MHA surfaces and 5 μL of the dissolved test compound was added to the discs, making the total amount of trial compound 10 μg/disc. Each plate contained two different types of standard anti-biotic paper discs, chloramphenicol (30 μg/disc) and tetracycline (30 μg/disc), which served as positive controls, one disc served as the negative control (5 μL MHB), one disc served as solvent control (5 μL DMSO) and two discs were used to evaluate the anti-bacterial property of the trial compound. The plates were incubated for 24 h at 37 °C. The anti-bacterial activity was evaluated by measuring the diameter of inhibition zones. Each experiment was performed in triplicate.

2.5.3. Determination of minimum inhibitory concentration (MIC) and minimum bactericidal concentration (MBC)

A broth micro-dilution method was used to determine the MIC and MBC values of the test compounds using CLSI protocols. Each test compound (5 μL) was added into the wells of a 96-well microplate containing 10^5 CFU/mL exponentially growing bacterial cells. The 96-well microplates were incubated at 37 °C for 24 h. The final tested concentrations ranged from 0.045 to 100 mg/mL. All tests were performed in triplicate. Four controls comprising medium with standard anti-biotics, chloramphenicol and tetracycline (positive control), medium with DMSO (solvent control), medium with inoculum bacterial cells (negative control) and medium with broth only (negative growth control) were included in each test. As an indicator of bacterial growth, 50 μL of 0.2 mg/mL *p*-iodonitrotetrazolium violet (Sigma-Aldrich) was added into each well; the presence of bacterial activity will convert the dye from colourless to purple. The microplates were further incubated for at least 30 min under aerobic agitation. The MIC was determined as the lowest concentration at which there is no trace of purple. After MIC determination, an aliquot of 100 μL from each well which showed no visible growth was spread onto MHA and further incubated at 37 °C for 24 h. The MBC was defined as the lowest concentration of the tested compound that produced a 99.9% reduction in bacterial viable count on MHA.

2.5.4. Time-kill assay

Time-kill assays were performed using the broth macro-dilution method in accordance with the CLSI guidelines. Inoculum suspensions with approximately 10^5 CFU/mL of exponentially growing bacterial cells were used in this study. The test compound (100 μL) was added to 10 mL of inoculum suspensions with final concentrations corresponding to ½ × MIC, 1 × MIC and 2 × MIC as determined earlier. A growth control comprising the bacterial strain without the test compound was included in each trial. The inoculum cultures were incubated at 37 °C on an orbital shaker at 200 rpm. A total of 200 μL was removed from each inoculum culture after time intervals of incubation (0, 1, 2, 3, 4, 8 and 24 h) and ten-fold serial dilutions were prepared in 0.85% normal saline. The numbers of viable cells were determined by the plate count technique which involved plating 25 μL of each dilution on a MHA plate. All plates were incubated at 37 °C for 24 h. The experiments were performed in triplicate. Data were analysed as killing curves by plotting the log_{10}[colony forming unit per millilitre (CFU/mL)] versus time (h), and the change in bacterial number was determined. The viable bacterial cell count for the time-kill end point determination, e.g.

Table 1
Crystal data and refinement details for **1**–**4**.

Compound	1	2	3	4
Formula	$C_{46}H_{86}Ag_2N_2P_2S_4$	$C_{46}H_{82}Ag_2N_2P_2S_4$	$C_{46}H_{86}Ag_2N_2O_4P_2S_4$	$C_{44}H_{82}Ag_2N_2O_2P_2S_4$
Formula weight	1073.08	1069.05	1137.08	1077.03
Crystal colour	Colourless	Colourless	Colourless	Colourless
Crystal size/mm^3	0.12 × 0.12 × 0.15	0.06 × 0.07 × 0.11	0.05 × 0.08 × 0.09	0.03 × 0.06 × 0.09
Crystal system	Triclinic	Triclinic	Triclinic	Triclinic
Space group	$P\bar{1}$	$P\bar{1}$	$P\bar{1}$	$P\bar{1}$
a/Å	9.9960(2)	11.57530(10)	10.42860(10)	10.3452(2)
b/Å	11.1286(2)	12.37100(10)	11.31020(10)	14.5439(2)
c/Å	12.4674(3)	18.7114(2)	11.8927(2)	16.9693(2)
α/°	105.922(2)	97.6640(10)	107.0080(10)	75.4140(10)
β/°	98.259(2)	106.9900(10)	96.4390(10)	89.6250(10)
γ/°	99.0760(10)	98.7240(10)	101.4560(10)	86.6510(10)
V/Å^3	1291.22(5)	2487.70(4)	1292.79(3)	2466.60(7)
Z	1	2	1	2
D_c/g cm^{-3}	1.380	1.427	1.461	1.450
$F(000)$	564	1120	596	1128
μ(Cu $K\alpha$)/mm^{-1}	8.409	8.729	8.493	8.838
Measured data	32,683	59,421	32,765	62,963
θ range/°	3.8–75.3	3.7–67.1	4.0–75.3	3.2–75.3
Unique data	5351	8901	5340	10,179
Observed data ($I \geq 2.0\sigma(I)$)	5332	8311	5174	9416
No. parameters	255	515	277	568
R, obs. data; all data	0.016; 0.041	0.024; 0.059	0.017; 0.041	0.032; 0.081
a; b in weighting scheme	0.019; 0.609	0.027; 2.256	0.017; 0.643	0.045; 2.033
R_w, obs. data; all data	0.016; 0.041	0.026; 0.061	0.018; 0.042	0.035; 0.084
Range of residual electron density peaks/eÅ^{-3}	−0.38–0.31	−0.61–1.15	−0.39–0.41	−1.32–1.15

bactericidal activity, is defined as a reduction of $\geq 3\log_{10}(CFU/mL)$ relative to the initial inoculum, whereas the bacteriostatic activity corresponds to $< 3\log_{10}(CFU/mL)$ decrease relative to the initial inoculum.

2.5.5. Cell viability assay

The cytotoxicity effects of the test compounds were evaluated using a normal cell line, i.e. human embryonic kidney cells (HEK 293). The HEK 293 cells were seeded in a 96-well plate with a density of 1×10^5 cells to a final volume of 100 μL per well. The test compounds were prepared by dissolution in DMSO to a concentration of 12 mg/mL, further diluted in Roswell Park Memorial Institute (RPMI)-1640 medium and then added to the well to obtain a final concentration of 0 (untreated control), 0.2, 0.4, 0.6, 0.8, 1 and 0.12 mg/mL. The treated HEK 293 cells were then incubated for 24 h. To investigate the cytotoxicity value of the test compounds, 20 μL of MTT (3-[4,5-dimethylthiazol-2-yl]-2,5-diphenyl tetrazolium bromide) solution (5 mg/mL in phosphate-buffered saline (PBS)) was added to each well and the plate was further incubated for 4 h at 37 °C. Prior to analysis, the medium was discarded and replaced with DMSO to dissolve the formazan crystals (i.e. the reduced form of MTT, (E/Z)-5-[4,5-dimethylthiazole-2-yl]-1,3-diphenylformazan) that had formed. The absorbance was measured at 570 nm through microplate reader (Tecan Infinite-M200). The 50% inhibitory concentration (IC_{50}) of each test compound was determined by plotting the graph of percentage of surviving cells against the concentration of the test compound. The assay was performed in triplicate.

3. Results and discussion

3.1. Chemistry and X-ray crystallography

The bis{tricyclohexylphosphanesilver(I) dithiocarbamate} compounds, **1**–**4**, Fig. 1, were prepared in good yield employing the metathesis reaction between AgNO$_3$ and the respective dithiocarbamate salt in the presence of Cy$_3$P. The colourless compounds are air- and light-stable for at least a month; spectroscopic data are collated in Section 2.3. The IR spectra featured the anticipated bands due to

$\nu(C-N)$ and $\nu(C-S)$ of the dithiocarbamate ligands. The expected resonances and integration were observed in the ^{1}H NMR. Similarly, the expected resonances were observed in the ^{13}C{^{1}H} spectra. Doublets were observed in all ^{31}P{^{1}H} spectra due to $J_{P\text{-}Ag}$ coupling, and in all spectra but that of **3**, these were resolved owing to coupling with the individual ^{107}Ag/^{109}Ag nuclei. The $J_{P\text{-}Ag}$ coupling constants for **1**–**4** are in close agreement with those reported for related phosphanesilver(I) complexes [32]. The stabilities of **1**–**4** were monitored by ^{31}P{^{1}H} NMR. Compounds **1** and **2** were not particularly soluble in d$_6$-DMSO and hence, their stability over time could not be reliably determined in this medium. By contrast, **3** and **4** were stable in d$_6$-DMSO solution for at least three days. Additional stability experiments were performed in CDCl$_3$ solution, again using ^{31}P{^{1}H} NMR. While **1** was stable for at least three days, some decomposition and precipitation was evident for **2**–**4** after the egress of time with the most noteworthy feature being the appearance of a resonance due to tricyclohexylphosphane oxide (Cy$_3$P═O) at approximately 50 ppm. Based on integration, approximately 5–10% decomposition had occurred after 24 h; spectra are given in Supplementary materials Fig. S1.

Crystals suitable for X-ray crystallography were obtained for **1**–**4**. The molecular structure of **1**, is located about a centre of inversion, is shown in Fig. 2a. The structure features a μ$_2$-bridging dithiocarbamate ligand whereby the S1 atom bridges two silver(I) centres with disparate Ag—S1 bond lengths of 2.5781(3) and 2.8334(3) Å, and with the S2 atom [2.5976(3) Å] closes a four-membered AgS$_2$C chelate ring. The participation of the S1 atom in two Ag—S bonds results in an elongation in the C1—S1 bond compared with the C1—S2 bond, i.e. 1.7333(13) vs 1.7136(13) Å. The four-coordinate geometry for silver is completed by the phosphane-P atom which forms the shortest of the four bonds to silver [2.4148(3) Å]. The PS$_3$ donor set is highly disordered with the angles ranging from an acute 66.585(9)° for the S1—Ag—S2 chelate angle to a wide 121.668(11)° for S1—Ag—P1. The Ag$_2$C$_2$S$_4$ atoms have the arrangement of a step ladder, with the chelate rings lying above and below the central Ag$_2$S$_2$ rectangle. Finally, the transannular Ag⋯Ag separation is 2.96470(19) Å.

The molecule in **2**, which lacks the crystallographic symmetry of **1**, is shown in Fig. 2b; selected interatomic parameters are given in the figure caption. In **2**, a major structural reorganisation has occurred in that the dithiocarbamate ligands lie to the same side of the central
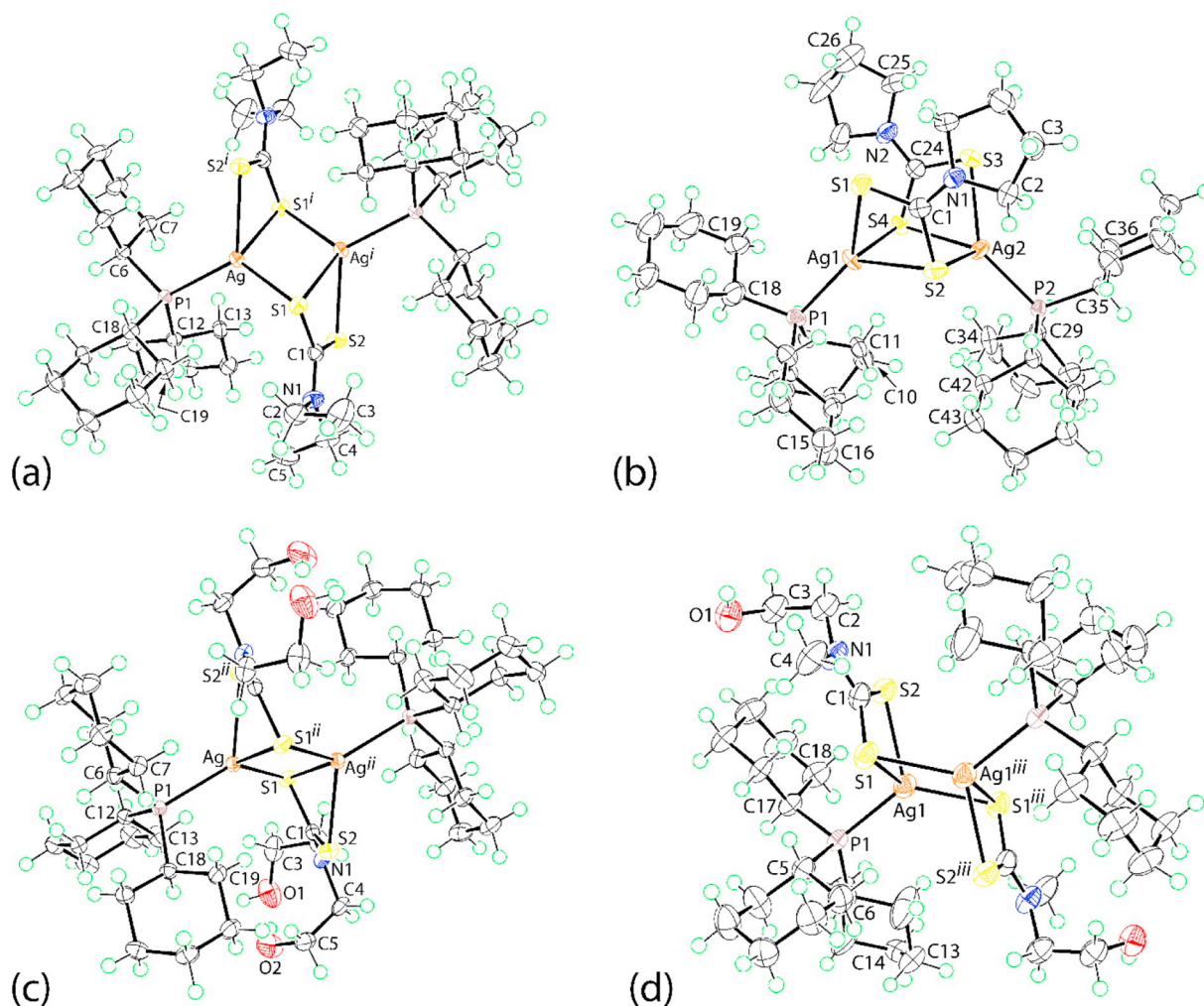
Fig. 2. Molecular structures of (a) centrosymmetric **1**; symmetry operation (i) 1 − x, 2 − y, 1 − z, (b) **2**. Selected geometric parameters: Ag1−S1 = 2.571(2), Ag1−S2 = 2.779(3), Ag1−S4 = 2.6742(19), Ag1−P1 = 2.327(2), Ag2−S3 = 2.5452(5), Ag2−S4 = 2.6796(5), Ag2−S2 = 2.7128(5) and Ag2−P2 = 2.3691(5) Å, (c) centrosymmetric **3**; symmetry operation (ii) −x, −y, 1 − z. Selected geometric parameters: Ag−S1 = 2.5574(4), Ag−S1^{ii} = 2.9920(5), Ag−S2^{ii} = 2.6054(4), Ag−P1 = 2.4239(4), Ag⋯Ag^{ii} 2.9287(2) Å and (d) the first crystallographically independent and centrosymmetric molecule of **4**; symmetry operation (iii) −x, 1 − y, 1 − z. Selected geometric parameters: Ag1−S1 = 2.9856(7), Ag1−S1^{iii} = 2.5446(6), Ag1−S2 = 2.5818(7), Ag1−P1 = 2.4197(6), Ag1⋯Ag1^{iii} 2.9014(4) Å; S1−Ag1−S2 = 64.848(19), S1−Ag1−P1^{iii} = 125.37(2)°.

Ag$_2$S$_2$ rectangle so that the arrangement of Ag$_2$C$_2$S$_4$ atoms is a boat, cf. the step-ladder observed in **1**. The trends in the relative lengths of the Ag−S are also different so that the central Ag$_2$S$_2$ core resembles a square, albeit being somewhat folded with the dihedral angle between the two Ag$_2$S planes being 13.94(4)°; the disparity in the C−S bonds persists as for **1**. The distortions from a regular tetrahedral geometry are greater in **2**. The most acute angle is still the chelate angle of 68.01(6)° [70.008(16) for the Ag2 centre] while the widest angle is 141.69(9)° formed by S1−Ag1−P1, i.e. involving the most tightly bound atoms; for the Ag2 centre, the equivalent angle, S3−Ag2−P2, is 139.685(18)°. A consequence of the reorganisation of the central core is an elongation in the Ag1⋯Ag2 separation in **2**, 3.617(2) Å cf. 2.96470(19) Å in **1**.

The molecular structure of centrosymmetric **3** follows that established for **1**, Fig. 2c, including the variations in the Ag−S and C−S bond lengths, and Ag⋯Ag separation. Similarly, the range of angles subtended at the Ag atom follow that observed in **1**, i.e. the chelate angle [55.109(11)°] is the most acute and the S1−Ag−P1 angle is the widest at 125.646(13)°. The final structure to be described is that of **4** for which the crystallographic asymmetric unit comprises two independent centrosymmetric molecules, i.e. two half molecules, Fig. 2d and Supplementary materials Fig. S2. Each of the independent centrosymmetric molecules adopts the same structural motif as found for **1** and **3**. The trends in the bond

lengths also follow those established above. A distinction between the molecules is found in the tetrahedral angles. While the trend in tetrahedral angles for the Ag1-containing molecule follow those seen for **1** and **3**, for the Ag2-molecule, the S3−Ag2−P2 and S4−Ag2−P2 are very similar, both being approximately 122°.

The molecular packing of **1** features cyclohexyl-methylene-C−H⋯S (dithiocarbamate) interactions whereby adjacent methylene-H atoms of a cyclohexyl ring bridge sulphur atoms derived from two different dithiocarbamate ligands of an adjacent binuclear molecule. These interactions lead to a supramolecular chain aligned along [1 0 0], Fig. 3a; chains pack without directional interactions between them, Supplementary materials Fig. S3; details of the geometric parameters characterising the interatomic parameters are given in the relevant figure captions of the Supplementary materials.

The only interaction between molecules identified within the standard distance criteria assumed in PLATON [31], is a C−H⋯π(chelate ring) interaction. Such C−H⋯π(chelate ring) interactions are now well known in the supramolecular chemistry of metal complexes, including those of dithiocarbamates, owing to the high delocalisation of π-electron density in the MS$_2$C chelate rings formed by dithiocarbamate ligands [33–35]. As illustrated in Fig. 3b, the C−H⋯π(chelate ring) interactions connect binuclear molecules into a supramolecular dimer;
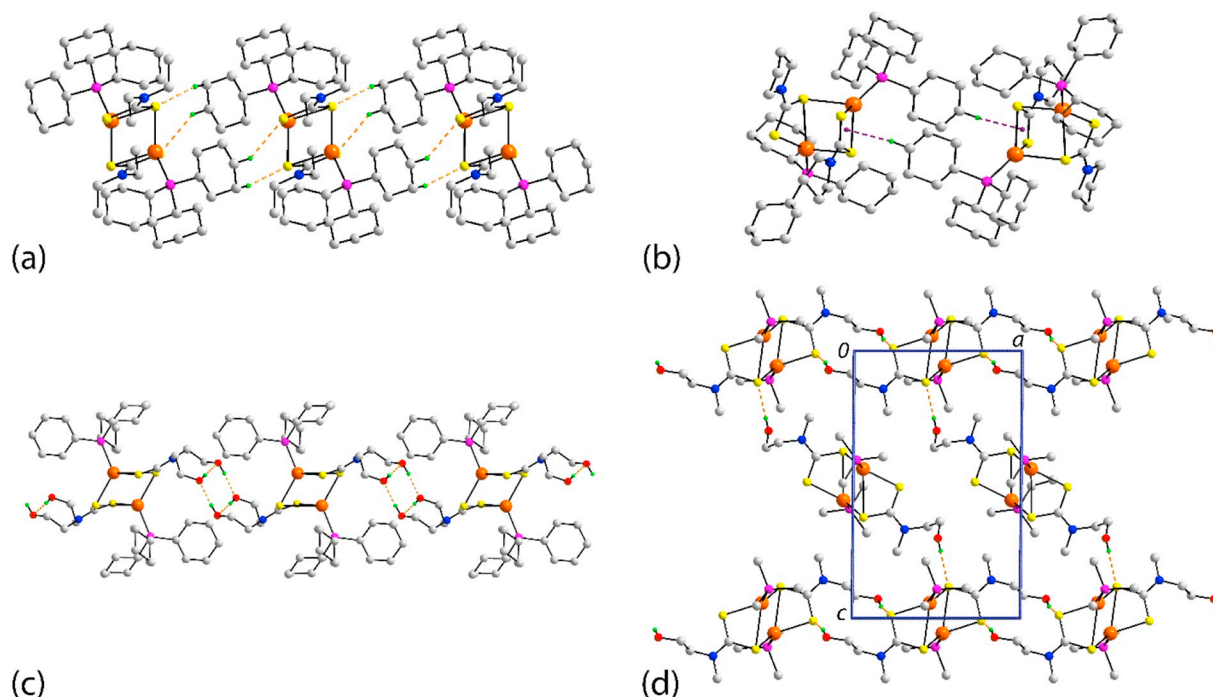
Fig. 3. Molecular packing in: (a) **1**, supramolecular chain parallel to the a-axis sustained by cyclohexyl-methylene-C−H···S(dithiocarbamate) interactions, shown as orange dashed lines, (b) **2**, supramolecular dimer sustained by cyclohexyl-methylene-C−H···π(Ag2,S3,S4,C24) interactions, shown as purple dashed lines, (c) **3**, supramolecular chain sustained by hydroxyl-O−H···O(hydroxyl) hydrogen bonding, shown as orange dashed lines and (d) **4**, supramolecular layer sustained by hydroxyl-O−H···S(dithiocarbamate) hydrogen bonding, shown as orange dashed lines; only the α-C carbon atoms of the cyclohexyl rings are shown. In each of (a)–(d), non-participating hydrogen atoms have been omitted for clarity.

these stack in columns parallel to the a-axis without directional interactions between them, Supplementary materials Fig. S4.

The presence of hydroxyl groups in each of **3** and **4** leads to the possibility of conventional hydrogen bonding in their crystals. In **3**, both intra- and inter-molecular hydroxyl-O−H···O(hydroxyl) hydrogen bonds are formed, leading to centrosymmetric eight-membered {···HO}$_4$ synthons and supramolecular chains along [1 1 0], Fig. 3c. The chains are connected into a supramolecular layer in the ab-plane by cyclohexyl-methylene-C−H···O(hydroxyl), S(dithiocarbamate) interactions as shown in Supplementary materials Fig. S5a; the layers stack along the c-axis without specific interactions between them, Supplementary materials Fig. S5b. In the crystal of **4**, rather than hydroxyl-O−H···O(hydroxyl) hydrogen bonds, hydroxyl-O−H···S(dithiocarbamate) hydrogen bonds are formed instead. As shown in Fig. 3d and Supplementary materials S6a, these sustain centrosymmetric 14-membered {···HOC$_2$NCS}$_2$ synthons which alternate with the Ag$_2$C$_2$S$_4$ rings along the a-axis and, at the same time contribute to much larger 50-membered {···SAgS···HOC$_2$NCS···HOC$_2$NCSAgSCNC$_2$OH}$_2$ synthons incorporating six hydroxyl-O−H···S(dithiocarbamate) hydrogen bonds and aligned along the c-axis. The resulting supramolecular layers stack along the b-axis without directional interactions between them Supplementary materials Fig. S6b.

An evaluation of the Cambridge Structural Database (CSD) [36] indicates there are seven structures available in the literature of the general formula [R$_3$PAg(S$_2$CNRR′)]$_2$ for R, R′, R″ = alkyl or aryl. There are no literature precedents with Cy$_3$P as the phosphane ligand nor one with pyrrolidinedithiocarbamate. It is noted that each of the known structures [37–41] adopts the step-ladder structural motif as described above for **1**, **3** and **4**. Interestingly, there are four structures of the analogous copper(I) derivatives. Consistent with the above, each of the binuclear structures of [R$_3$PCu(S$_2$CNEt$_2$)]$_2$ for R = Me, Et and OMe [42] is centrosymmetric implying a step-ladder motif. However, the recently described structure of {Cy$_3$PCu[S$_2$CN(CH$_2$)$_4$]}$_2$ [43], i.e. directly analogous to **2**, adopts the same boat form as for **2**. Clearly,

systematic structural studies are required to ascertain the reason(s), e.g. steric and/or electronic, for these structural variations.

In terms of related structures with tetrahedrally-coordinated silver within a PS$_3$ donor set, there are over 100 examples included in the CSD [36]. However, there is only a sole example having Cy$_3$P as the phosphane ligand, namely Cy$_3$PAg[(phenyl-tris(3-methyl-2-thioxoimidazol-1-yl)borate-S,S′,S″)] [44]. In this structure, with two independent molecules in the asymmetric unit, the Ag−P bond lengths are experimentally equivalent at 2.3958(7) and 2.3980(7) Å, whereas the Au−S bond lengths span a range 2.5692(8) to 2.6530(9) Å. In the structures of **1**, **3** and **4**, where the central ring adopts the conformation of a step-ladder, the Ag−P bond lengths are systematically longer and the Ag−S bond lengths span a greater range that the literature structure, observations traced to the steric crowding in the molecules. For **2**, the Ag−P bond length is marginally shorter than those in the literature structure and the Ag−S bond lengths span a similar range of values.

3.2. Anti-bacterial activity

For all biological trials, only freshly prepared solutions were used. The Kirby-Bauer disc diffusion method was used in the initial screening for the anti-bacterial properties of dithiocarbamate ligands, **1–4**, AgNO$_3$ and standards (Table 2). The solvent used in this study, i.e. DMSO, did not produce an inhibition zone, suggesting DMSO does not exert anti-bacterial effects on the tested bacterial strains. The results also showed that the $^-$S$_2$CNR(CH$_2$CH$_2$OH) anions, for R = CH$_2$CH$_2$OH and Me, do not have anti-bacterial activity against the tested bacterial strains while the $^-$S$_2$CNEt$_2$ anion showed low activity, having an effect on only one Gram-positive bacterium (*S. epidermidis*), but not Gram-negative bacteria. By contrast, the $^-$S$_2$CN(CH$_2$)$_4$ anion was mildly active against all Gram-positive bacteria and one Gram-negative bacteria (*K. pneumoniae* ATCC 13883).

Enhanced anti-Gram positive bacterial activity was observed when each of the dithiocarbamate anions were incorporated in the silver

Table 2

Anti-bacterial activity measured by zone of inhibition (mm) of the dithiocarbamate anions, **1–4** and AgNO₃ (10 μg/disc) and standard anti-biotics (30 μg/disc).[a,b,c]

Microorganism	⁻S₂CNEt₂	1	⁻S₂CN(CH₂)₄	2	3	4	AgNO₃	Tetracycline	Chloramphenicol
Gram-positive bacteria									
E. faecalis ATCC 33186	-	7	7	8	7	7	7	39	31
S. aureus (MRSA) MTCC 381123	-	-	7	-	9	7	7	30	28
S. epidermidis ATCC 700576	7	9	7	8	9	10	8	38	38
S. pneumoniae ATCC 49619	-	8	7	8	9	8	8	34	30
S. pyogenes ATCC 49399	-	8	7	9	10	12	9	30	33
Gram-negative bacteria									
E. coli ATCC 11775	-	-	-	-	-	-	8	22	26
E. coli MTCC 710859	-	-	-	-	-	-	8	25	31
K. pneumoniae ATCC 13883	-	-	7	-	-	-	8	25	31
K. quasipneumoniae ATCC 700603	-	-	-	-	-	-	8	17	15
P. aeruginosa ATCC 10145	-	-	-	-	-	-	7	13	11
P. mirabilis ATCC 25933	-	-	-	-	-	-	7	10	25
S. enterica ATCC 14028	-	-	-	-	-	-	7	28	31

[a] The diameter of inhibition zones in millimetres were measured around the discs after 24 h incubation; -, no zone of inhibition.

[b] The dithiocarbamate anions ⁻S₂CN(CH₂CH₂OH)₂ and ⁻S₂CN(Me)CH₂CH₂OH did not exhibit inhibition.

[c] The presented zones of inhibition are the minimum zones obtained from three independent experiments conducted in triplicate.

compounds, **1–4**; **1–4** exhibited no activity against Gram-negative bacteria. Comparing the R = alkyl species, **1** and **2**, **2** tends to be marginally more potent than **1** exhibiting anti-bacterial effects against all Gram positive bacteria, except for *S. aureus* (MRSA). The differences in potency exhibited by **1–4** against the Gram-positive bacteria were generally small with the exception against *S. pyogenes*. *S. pyogenes*, an α-haemolytic bacterium implicated in *Streptococcal pharyngitis*, also known as Strep Throat, appeared to be the most susceptible among the tested clinically important Gram-positive bacteria [45]. Despite *S. pyogenes* being an important medical pathogen, its biology, such as integrity of cell wall, the presence of efflux pumps (that can pump out anti-bacterial agents), etc. is not well documented [45] so the apparent enhanced efficacy of **1–4** is of interest and worthy of further investigation. Compared with **1** and **2**, the derivatives with CH₂CH₂OH substituents were generally more potent with **3** being the most active among the series against *S. pneumoniae* (9 mm) and **4** being most potent against both *S. pyogenes* (12 mm) and *S. epidermidis* (10 mm). Crucially, both **3** and **4** exhibit anti-bacterial activity against *S. aureus* (MRSA) with inhibition zones of 9 and 7 mm, respectively.

The disc diffusion results demonstrated that compounds **1–4** were specifically effective against Gram-positive bacteria but not Gram-negative bacteria. The selective activity against only Gram-positive bacteria leads to the speculation that the permeability barrier of the outer membrane present in Gram-negative bacteria limits the entry of compounds **1–4**. The Gram-negative cell outer membrane contains lipopolysaccharides in its outer leaflet and phospholipid in its inner leaflet that are known to effectively exclude several drugs compared to Gram-positive bacteria [46]. Similar anti-bacterial selectivity effects were observed for the previously studied silver, copper and gold dithiocarbamates [22–24].

Trials were also conducted on AgNO₃. It is interesting to note that AgNO₃ was non-specific in terms of inhibiting Gram-positive and Gram-negative bacteria indicating the presence of the dithiocarbamate ligands in **1–4** introduces specificity in activity. The clinically-employed anti-biotics chloramphenicol and tetracycline (each 30 μg/disc) were included in this study as controls. These drugs produced respectively, large inhibition zones of 30–39 and 28–38 mm against Gram-positive bacteria, and 10–28 and 11–31 mm against Gram-negative, Table 2. These differences in activity against Gram-positive bacteria are largely due to the lower concentrations employed for **1–4** (10 μg).

3.3. Determination of minimum inhibitory concentration (MIC) and minimum bactericidal concentration (MBC)

The disc diffusion assay showed that two of the dithiocarbamate anions and **1–4** exhibited anti-bacterial activity. This activity was further quantitatively evaluated against Gram positive bacteria by determining their MIC and MBC values with the results tabulated in Table 3; the anti-biotics tetracycline and chloramphenicol were used as positive controls.

In this study, **1–4** and dithiocarbamate ligands were not effective against the tested Gram negative bacteria, except for the ⁻S₂CN(CH₂)₄ anion against *K. pneumoniae*; this gave an MIC value of 100 μg/mL and was not studied further. The other active anion, ⁻S₂CNEt₂, exhibited anti-bacterial effects against only one Gram-positive bacterium, *S. epidermidis*, with an MIC value of 100 μg/mL and again this was not studied further. For ⁻S₂CNR(CH₂)₄, MIC values ranging from 12.5 to 50.0 μg/mL were observed for all Gram-positive bacteria. The anti-bacterial effects of **1–4** were maintained or enhanced when compared to their respective anions, except for **2** on *S. aureus* (MRSA). The enhanced inhibitory effects of **1–4** compared to the (charged) dithiocarbamates might be due to an increase in the lipophilicity of (neutral) **1–4** [47,48]. The MIC values of **1–4** were in the range of 0.10–100 μg/mL, whereas tetracycline was active in the range of 0.20–0.39 μg/mL and chloramphenicol in the range of 1.56 to 6.25 μg/mL.

As a general observation, the MIC values of **3** and **4** against all tested Gram-positive bacteria were lower than for **1** and **2**, and significantly lower than those produced by AgNO₃. Compound **3** was effective in inhibiting the growth of all tested Gram-positive bacteria with MIC values in the range of 0.39 (*S. epidermidis* and *S. pneumoniae*) to 3.13 μg/mL (*S. aureus* (MRSA)). Compound **4** was the most effective compound across the series, being most potent against *S. epidermidis* with a MIC value of 0.10 μg/mL. It was also the most active against *S. pneumoniae* (MIC = 0.20 μg/mL), *E. faecalis* (0.78 μg/mL), *S. pyogenes* (0.78 μg/mL) and *S. aureus* (MRSA) (1.56 μg/mL).

It was initially expected that **3**, Cy₃PAg[S₂CN(CH₂CH₂OH)₂], with two hydroxyethyl groups, would be the most effective anti-bacterial agent as the second hydroxyethyl functional group might allow for the formation of additional hydrogen bonding interactions with biological substrates, leading to the impairment of normal cellular processes in bacterial cells [49]. However, the results showed **4**, Cy₃PAg[S₂CN(Me)CH₂CH₂OH], with a less polar group (methyl), was most active. It is possible that the increased lipophilic character of **4** enables more efficient diffusion across the membrane into the cytoplasm of bacterial cells, before exhibiting its anti-bacterial effects [50].

Previous studies on a related gold(I) species, i.e. Cy₃PAu[S₂CN(CH₂CH₂OH)₂], gave MIC values in the range of 1.56–50.00 μg/mL against all tested Gram-positive bacteria [24]. In the present study, the MIC values obtained for compound **3**, {Cy₃PAg[S₂CN(CH₂CH₂OH)₂]}₂ were relatively lower than the MIC values for the aforementioned gold

Table 3
MIC (μg/mL) and MBC (μg/mL) of $^-S_2CN(CH_2)_4$, 1–4, AgNO₃, tetracycline and chloramphenicol against Gram-positive bacteria.[a,b]

	1		$^-S_2CN(CH_2)_4$		2		3		4		AgNO₃		Chloramphenicol		Tetracycline	
	MIC	MBC/MIC	MIC	MBC/MIC	MIC	MBC/MIC	MIC	MBC/MIC	MIC	MBC/MIC	MIC	MBC/MIC	MIC	MBC/MIC	MIC	MBC/MIC
E. faecalis ATCC 33186	100.00	ND	25.00	1	25.00	ND	1.56	1	0.78	1	25.00	2	3.13	16	0.20	63
S. aureus (MRSA) MTCC 381123	-	NA	12.50	ND	-	NA	3.13	2	1.56	2	25.00	ND	6.25	ND	0.39	32
S. epidermidis ATCC 700576	12.50	1	12.50	2	3.13	1	0.39	2	0.10	2	25.00	2	1.56	32	0.39	4
S. pneumoniae ATCC 49619	100.00	ND	50.00	ND	50.00	ND	0.39	16	0.20	16	25.00	2	3.13	16	0.20	31
S. pyogenes ATCC 49399	12.50	1	25.00	1	6.25	1	1.56	1	0.78	1	25.00	2	1.56	4	0.20	16

[a] MIC: minimum inhibitory concentration (μg/mL); MBC: minimum bactericidal concentration (μg/mL); MBC/MIC: MBC/MIC ratio for bacteriostatic or bactericidal activity; -: MIC > 100 μg/mL; *NA*: not applicable; *ND*: not determined as the bacterium had grown across all tested dilutions (MBC > 100 μg/mL).

[b] The presented MIC values are the lowest inhibitory concentrations obtained from three independent experiments conducted in triplicate.

derivative. This, coupled with observation that replacing one hydroxyethyl with a methyl group to yield **4** further enhanced the anti-bacterial activity, indicate that the new silver dithiocarbamates described herein are potential potent anti-bacterial agents.

Given that inhibition of bacterial growth does not necessarily indicate the ability of a test compound to kill a particular bacterium, the minimum bactericidal concentration (MBC) was determined to identify whether the test compound was able to kill a bacterium (bactericidal) or only inhibited growth (bacteriostatic). Both bactericidal and bacteriostatic anti-biotics are used to treat a variety of bacterial infections. Bactericidal anti-biotics can be taken for a short period of time and are often used to reduce the risk/cure the infection better than bacteriostatic anti-biotics. It is noted that bacteriostatic anti-biotics are often sufficient to treat an infection by slowing the growth of the bacteria while the individual's immune system fights/eliminates the infection. However, the infection may persist if a patient is immunocompromised [51,52]. The knowledge on the use of either bactericidal or bacteriostatic agents is crucial for the effective treatment of an infected patient. With this in mind, the bactericidal or bacteriostatic properties of **1–4** were investigated.

The generally accepted definition of MBC by Levison [53] is used herein: an anti-bacterial agent is considered bactericidal if the value of MBC is not more than four-fold greater than the MIC, i.e. MBC/MIC ≤ 4. The anti-bacterial properties of **1–4** against susceptible strains were analysed by the MBC assay and the results are summarised as MBC/MIC ratios in Table 3. For the chosen Gram-positive bacteria, chloramphenicol (see below) and tetracycline were bacteriostatic. While AgNO₃ was bactericidal against all tested bacteria, this is not potent. For compounds **1** and **2**, bactericidal activity was proven against *S. pyogenes* and *S. epidermidis*. Compounds **3** and **4** were shown to be bactericidal (MBC/MIC ≤ 2) toward all the susceptible Gram-positive strains, except against *S. pneumoniae*, with the MBC being 16-fold greater than the MIC, indicating these are bacteriostatic. These results indicate that the bactericidal and bacteriostatic activities of **1–4** are dependent on the bacterial strain. This behaviour is similar to standard anti-biotic, chloramphenicol which is considered bacteriostatic against most Gram-positive and many Gram-negative aerobic bacteria by binding to the 50S subunit of the bacterial 70S ribosome which causes inhibition of protein synthesis [54]. However, bactericidal activity on some bacteria, such as *H. influenzae*, *S. pneumoniae* and *N. meningitidis*, has also been reported which enables the use of chloramphenicol in the treatment of meningitis caused by the mentioned pathogens [55]. Similar variable bactericidal/bacteriostatic activities were also reported for related phosphanegold(I) dithiocarbamates [23].

Disc diffusion and MIC are two standard assays used in the determination of anti-bacterial properties. The presence of a zone of inhibition indicates anti-bacterial potential and it is expected MIC tests would support the results. However, in this present study, a positive correlation was not observed for these two independent experiments. For instance, based on the MIC results, at 0.10 μg/mL, **4** was shown to be the most effective against *S. epidermidis*, but **4** only produced a 10 mm of zone of inhibition against *S. epidermidis* while the comparable result against *S. pyogenes*, with a MIC value of 0.78 μg/mL, has a zone of inhibition of 12 mm. Comparing the two assays, disc diffusion makes use of solid media while MIC uses liquid media. It is thought that the diffusion and mobility of the silver compounds in the solid medium is restricted, leading to poor diffusion through agar medium and thus moderate zones of inhibition are observed. Similar observations were made for related tin dithiocarbamates [50].

3.4. Time kill assay

Time kill assays provide useful information to describe the pharmacodynamics of trial anti-bacterial compounds [56]. In contrast to MIC determinations, which involve the study of the anti-bacterial effect at one concentration after a specific time, the time kill assay

Table 4
Summary of in-vitro time-kill assay of **1–4** against susceptible pathogen strains.

Microorganism	Compound	Log$_{10}$ CFU/mL[a]														
		½ × MIC					1 × MIC					2 × MIC				
		1 h	2 h	4 h	8 h	24 h	1 h	2 h	4 h	8 h	24 h	1 h	2 h	4 h	8 h	24 h
E. faecalis ATCC 33186	**1**	+0.1	+0.1	+1.0	+3.3	+3.4	0.0	−0.1	+1.0	+3.2	+3.3	−0.2	−0.2	+0.8	+3.1	+3.3
	2	−0.1	+0.1	+0.8	+3.2	+3.5	−0.1	−0.1	+0.3	+2.9	+3.4	−0.3	−0.1	+0.1	+2.0	+3.4
	3	−0.8	−0.5	−1.5	−1.5	+4.7	−0.8	−0.7	−4.4	−4.4	+4.6	−1.4	−0.9	−4.4	−4.4	+3.3
	4	−0.1	−0.4	0.0	+0.1	+3.5	−0.1	−4.7	−0.2	0.0	+3.5	−0.3	−4.7	−4.7	−4.7	+3.5
S. aureus (MRSA) MTCC 381123	**3**	−0.2	−0.1	−0.8	−0.6	+4.8	−0.3	−0.4	−2.2	−1.6	+2.7	−0.4	−0.6	−5.2	−2.2	+0.8
	4	−0.3	−0.4	+0.6	+2.7	+5.1	−0.3	−5.2	+0.1	+0.1	+3.0	−0.5	−5.2	−5.2	−0.9	+2.6
S. epidermidis ATCC 700576	**1**	+0.3	+0.3	+1.0	+1.2	+4.0	−3.3	+0.2	+0.7	+1.1	+3.9	−3.5	−3.5	+0.5	+1.0	+3.7
	2	+0.3	+0.3	+0.7	+1.2	+4.4	−3.5	0	+0.3	+0.9	+4.0	−3.5	−3.5	−0.2	+0.6	+3.5
	3	+0.1	+0.1	−0.2	0.0	+4.0	−0.3	−0.3	0.0	+0.2	+3.7	−0.5	−3.5	−0.5	−0.2	+3.4
	4	+0.3	0.0	+0.3	+1.1	+4.4	0.0	−3.3	0.0	+0.8	+4.0	−0.5	−3.5	−3.5	+0.5	+3.7
S. pneumoniae ATCC 49619	**1**	−0.2	−0.2	+0.5	+2.6	+4.0	−0.3	−0.6	+0.4	+2.5	+3.8	−4.1	−4.1	+0.3	+2.2	+3.4
	2	+0.1	+0.2	+0.4	+1.6	+4.1	+0.1	+0.1	+0.2	+1.4	+3.9	0.0	0.0	0.1	+1.1	+3.3
	3	−0.1	+0.1	+0.1	+1.7	+4.7	−0.1	0.0	0.0	+1.5	+4.8	−0.2	0.0	−0.1	+1.1	+4.6
	4	0.0	−0.1	+0.5	+2.4	+4.8	0.0	−0.3	+0.3	+2.2	+4.7	−0.6	−1.1	−0.2	+2.0	+4.6
S. pyogenes ATCC 49399	**1**	+0.1	0.0	+0.3	+1.2	+3.8	0.0	−1.0	−4.5	+0.5	+3.7	−0.1	−4.5	−4.5	−0.5	+3.6
	2	+0.1	+0.1	−0.7	+0.3	+3.9	+0.1	0.0	−4.5	−4.5	+3.8	−0.2	−0.1	−4.5	−4.5	+3.8
	3	−0.5	−0.2	−1.0	−0.5	+4.1	−0.8	−0.3	−3.8	−3.8	+4.2	−4.2	−4.2	−4.2	−4.2	+3.6
	4	−0.3	−1.0	−0.6	+0.1	+3.2	−4.4	−4.4	−4.4	−0.5	+2.9	−4.4	−4.4	−4.4	−1.4	+1.6

[a] Relative to log$_{10}$ CFU/mL of initial inoculum (a negative value indicates a reduction of bacterial cell number, and a positive value indicates an increase of bacterial cell number). Values shown are the mean of triplicate determinations from each experiment.

investigates the effect of three different concentrations of **1–4**, ½×, 1× and 2 × MIC, over a 24 h incubation period. According to CLSI protocols, a 3 log$_{10}$ CFU/mL or greater reduction in the viability of the bacterial colony relative to the initial inoculum is the point that differentiates between bactericidal and bacteriostatic activity [57]. The pharmacodynamics of **1–4** (Table 4 and Figs. 4–7) as well as chloramphenicol and tetracycline (Supplementary materials Table S1 and Figs. S7 and S8) against susceptible bacterial strains were determined using time kill assays; the standards were uniformly bacteriostatic against the tested bacteria.

As expected from the determined MBC/MIC ratios in Table 3, the time kill assays for **1** and **2** toward *E. faecalis* and *S. pneumoniae* at 1 × MIC indicated they were bacteriostatic whereas toward *S. epidermidis* and *S. pyogenes* exhibited bactericidal behaviour. At 1 × MIC, **1** and **2** were bactericidal toward *S. epidermidis* after 1 h, and after 4 h toward *S. pyogenes*. At 2 × MIC, **1** was bactericidal toward *S. epidermidis* and *S. pneumoniae* after 1 h, and after 2 h for *S. pyogenes*. The latter result indicated **1** demonstrates rapid concentration-dependent

bactericidal activity against *S. pyogenes*. Under the same conditions, **2** exhibited similar bactericidal effects as **1** toward *S. epidermidis* after 1 h at 2 × MIC. Compound **2** was also bactericidal toward *S. pyogenes* after 4 h at 2 × MIC. Therefore, the killing rate of **2** was slower than **1** against *S. pyogenes*.

The common feature of the time kill assays for **3** and **4** were that all were bactericidal against all bacteria with the notable exception of *S. pneumoniae*. Compound **3** demonstrated rapid concentration-dependent bactericidal activity against *S. pyogenes*. At 1 × MIC and 2 × MIC, bactericidal activity was achieved at 4 and 1 h, respectively, against *S. pyogenes*. By contrast, against *E. faecalis*, time to achieve 3 log$_{10}$ kill was similar at 1 × MIC and 2 × MIC. As a general observation, at 2 × MIC concentrations bactericidal effects were noted only after 4 h for *E. faecalis* and *S. aureus* (MRSA), 2 h for *S. epidermidis* and 1 h for *S. pyogenes*. Two of these, *E. faecalis* and *S. pyogenes*, were also susceptible at 1 × MIC after 4 h.

For **4**, the required time to achieve 3 log$_{10}$ kill was similar at 1 × MIC and 2 × MIC against *E. faecalis*, *S. aureus* (MRSA), *S.*
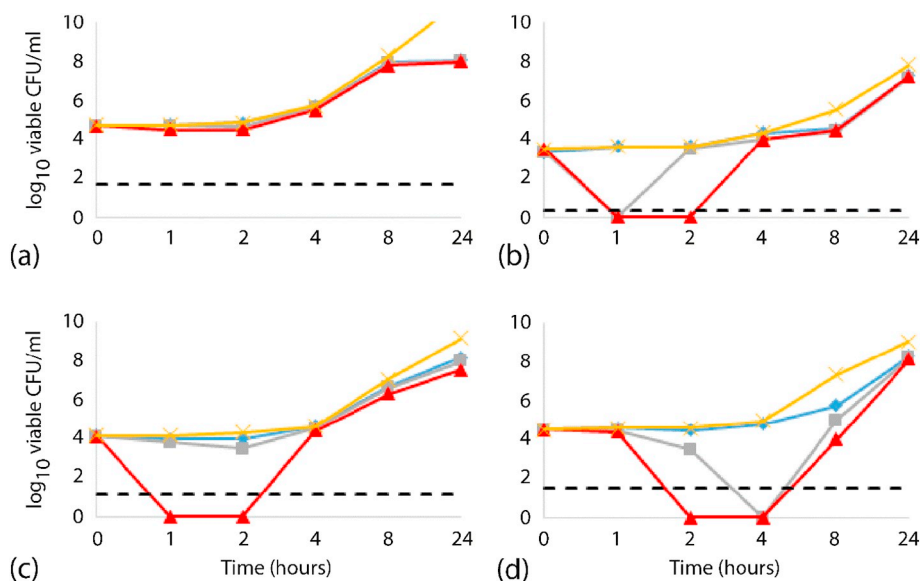

Fig. 4. Time kill curves for **1**: (a) *E. faecalis*, (b) *S. epidermidis*, (c) *S. pneumoniae* and (d) *S. pyogenes*. The bactericidal level is indicated by the dashed lines — negative control ×, ½ × MIC ♦, 1 × MIC ■ and 2 × MIC ▲.
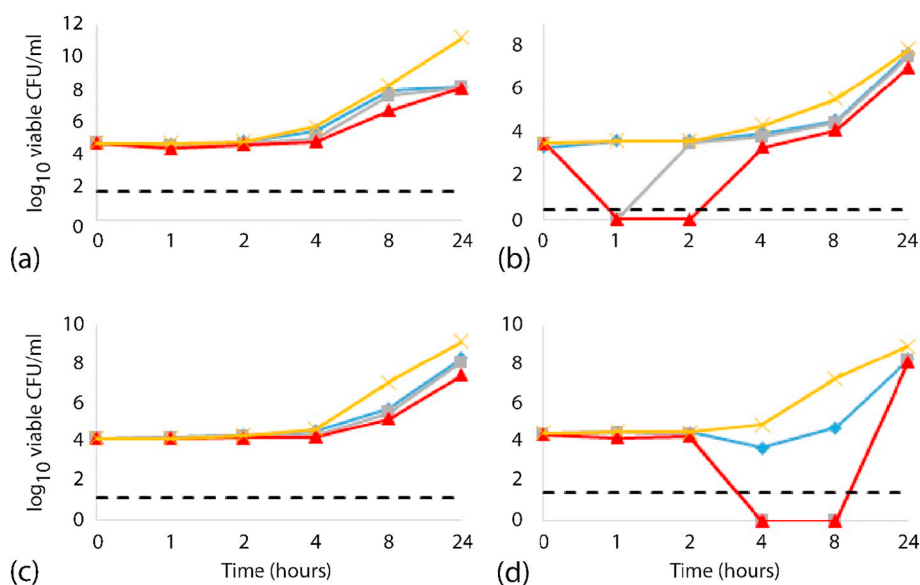
Fig. 5. Time kill curves for **2**: (a) *E. faecalis*, (b) *S. epidermidis*, (c) *S. pneumoniae* and (d) *S. pyogenes*. The bactericidal level is indicated by the dashed lines —, negative control ×, ½ × MIC ♦, 1 × MIC ■ and 2 × MIC ▲.

epidermidis (all 2 h) and *S. pyogenes* (1 h) at both 1 × MIC and 2 × MIC concentrations.

The emergence of the multi-drug resistant bacterium, *S. aureus* (MRSA), is recognised as a serious health threat to the general public by the Centers for Disease Control and Prevention (CDC) as this rapidly develops resistance to new anti-biotics. In 2011, Vidaillac et al. [58] examined the in vitro activity of three anti-biotics commonly used in the treatment of *S. aureus* (MRSA) infections, namely oritavancin, vancomycin and teicoplanin. It was reported that oritavancin exhibited rapid bactericidal activity against *S. aureus* (MRSA) at 4 × MIC after 9 h

exposure while both vancomycin and teicoplanin achieved a maximum 2.7 $\log_{10}$ CFU/mL decrease against *S. aureus* (MRSA) at 8 × MIC. In the present study, the kill kinetic profile of **4** showed a far more rapid bactericidal activity i.e. within 2 h at 2 × MIC, compared to oritavancin. Also, **4** reached a maximum 5.2 $\log_{10}$ CFU/mL decrease against *S. aureus* (MRSA) at 2 × MIC compared to vancomycin and teicoplanin. The killing rate of **4** was faster than **3** against *S. aureus* (MRSA) in which bactericidal activities were seen after 2 h to achieve a maximum 5.2 $\log_{10}$ CFU/mL decrease at 2 × MIC. These results underscore the promising utility of **3** and **4** as anti-bacterial agents.
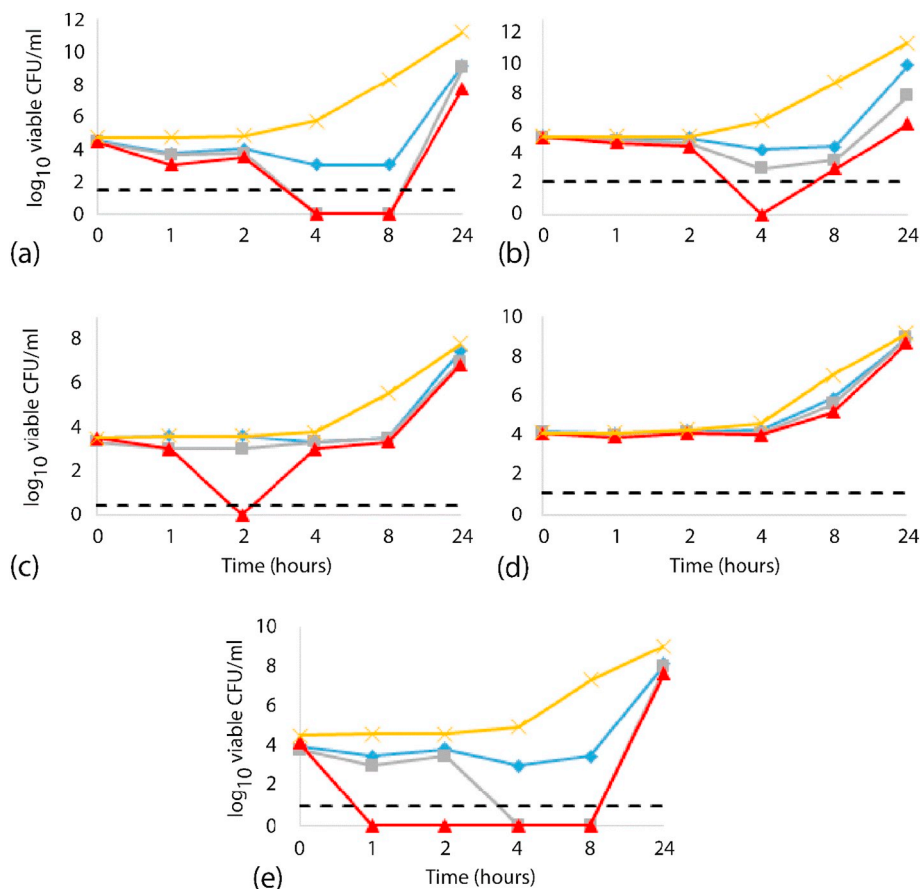

Fig. 6. Time kill curves for **3**: (a) *E. faecalis*, (b) *S. aureus (MRSA)*, (c) *S. epidermidis*, (d) *S. pneumoniae* and (e) *S. pyogenes*. The bactericidal level is indicated by the dashed lines —, negative control ×, ½ × MIC ♦, 1 × MIC ■ and 2 × MIC ▲.
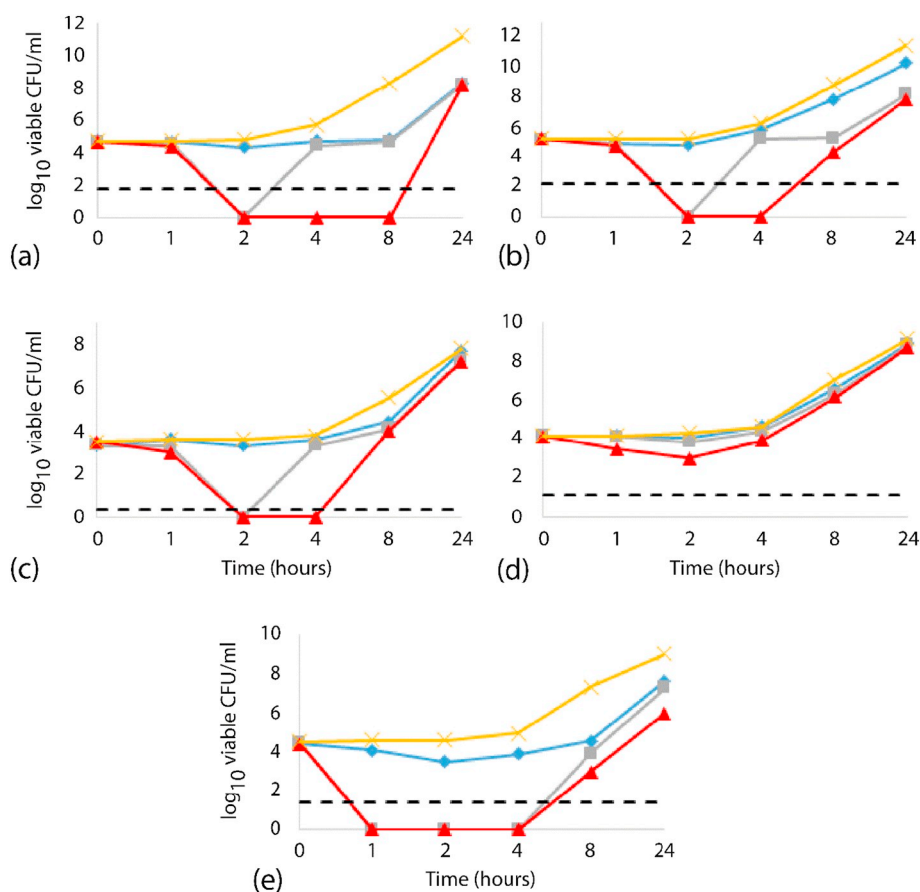
Fig. 7. Time kill curves for **4**: (a) *E. faecalis*, (b) *S. aureus* (MRSA), (c) *S. epidermidis*, (d) *S. pneumoniae* and (e) *S. pyogenes*. The bactericidal level is indicated by the dashed lines —, negative control ×, ½ × MIC ♦, 1 × MIC ■ and 2 × MIC ▲.

Notably, all strains were found to regrow to the same or almost the same level as the control after 24 h at concentrations of 2×, 1× and ½ × MIC. This phenomenon is common in studies of bacterial killing rate of anti-microbial agents in time kill assays [59]. This may be due to two different sub-populations with different susceptibility in which the selective growing of resistant sub-population take over the preferential killing of susceptible sub-population at specified time of interaction [56].

In summary, compounds **3** and **4** are demonstrated to be more effective anti-bacterial agents compared to **1**, **2** and AgNO₃. Silver nitrate, used in the synthesis of **1–4**, is a known an anti-septic agent used in the prevention of eye infections in the new-born children and is known to be active against both Gram positive and Gram negative bacteria [8]. Considering the chemical structures, charge-neutral **3** and **4** are significantly bulkier than the salt due to the presence of the tricyclohexylphosphane and dithiocarbamate ligands. These characteristics ease the diffusion of the compounds across the bacterial membrane before they exhibit their anti-bacterial activity. The additional hydroxyl group (s) in **3** and **4** impart significant effects in the anti-bacterial activity as compared to **1** and **2**, indicating that the ratio of hydrophobicity/hydrophilicity can be fine-tuned for the enhancement of in vitro anti-bacterial activity. To determine the lipophilicity and hydrophobic properties of the synthesised compounds, oil/water partition co-efficient (in term of logP) in systems such as octanol/water and chloroform/water can be further investigated [60]. The anti-bacterial activity of metal dithiocarbamates is suggested to arise by the inactivation of physiologically important enzymes [14,61]. Thus, possible mechanisms of action of **1–4** can be verified by investigating their inhibition of enzymes such as SH-protease papain, NADP + -dependent alcohol dehydrogenase and the NAD + -dependent alcohol dehydrogenase [62].

3.5. Cytotoxicity

The possible cytotoxic effects of **1–4** were investigated through a MTT assay conducted on a normal cell line, the HEK 293 human embryonic kidney epithelial cell line, as an in vitro representative of a normal cell model, at various concentrations, starting from 0, 8, 15, 30, 60 and 90 μM. The toxicity effects of **1–4** toward HEK 293 are presented in Supplementary materials Fig. S8. The results indicated the percentage of cell viability after 24 h treatment with **1–4** was observed at > 80% against the six concentrations. The IC₅₀ values were > 90 μM indicating **1–4** are non-cytotoxic.

4. Conclusions

Four new binuclear phosphanesilver(I) dithiocarbamates, **1–4**, have been characterised and investigated for their anti-bacterial potential. Based on MIC assays, **1–4** possess potent and selective anti-bacterial activity against Gram-positive pathogens; **1–4** are non-toxic to human embryonic kidney cells, HEK 293. Crucially, **3** and **4** are also potent against *S. aureus* (MRSA), which is resistant to several classes of antibiotics. While interesting selectivity is noted, **4**, with low MIC values and more rapid bactericidal activity against *S. aureus* (MRSA), could provide clinical advantages in bacteriostatic therapy for immunocompromised patients by rapid elimination of *S. aureus* (MRSA) pathogens and thereby reduce the possibility of the spread of infection. Based on the time-kill studies, the concentrations required and bacterial killing rates of **1–4** were different from each other suggesting distinct mechanisms of action. In summary, the new compounds show great promise as effective anti-bacterial agents against Gram-positive bacteria. In particular, further investigations are warranted to determine the therapeutic potential of compound **4** against *S. aureus* (MRSA).

Conflict of interest

The authors have no conflict of interest to disclose.

Acknowledgements

Appendix A. Supplementary data

Supplementary data to this article can be found online at https://doi.org/10.1016/j.jinorgbio.2018.12.017.

References

[1] J. Rai, G.K. Randhawa, M. Kaur, Int. J. Appl. Basic Med. Res. 3 (2013) 3–10.
[2] V.M. D'Costa, C.E. King, L. Kalan, M. Morar, W.W. Sung, C. Schwarz, D. Froese, G. Zazula, F. Calmels, R. Debruyne, G.B. Golding, H.N. Poiner, G.D. Wright, Nature 477 (2011) 457–461.
[3] Global Antimicrobial Resistance Surveillance System (GLASS) Report: early implementation, Url: World Health Organization, http://apps.who.int/iris/bitstream/handle/10665/259744/9789241513449-eng.pdf;jsessionid=7FE3181E45D73C9BC5343547BBAD2F71?sequence=1, (2016–2017) , Accessed date: 4 September 2018.
[4] W.R. Li, X.B. Xie, Q.S. Shi, H.Y. Zeng, Y.S. Ou-Yang, Y.B. Chen, Appl. Microbiol. Biotechnol. 85 (2010) 1115–1122.
[5] M. Gielen, E.R.T. Tiekink (Eds.), Metallotherapeutic Drugs and Metal-based Diagnostic Agents: The Use of Metals in Medicine, JohnWiley & Sons Ltd, Chichester, 2005.
[6] S. Silver, FEMS Microbiol. Rev. 27 (2003) 341–353.
[7] S. Medici, M. Peana, G. Crisponi, V.M. Nurchi, J.I. Lachowicz, M. Remelli, M.A. Zoroddu, Coord. Chem. Rev. 327 (2016) 349–359.
[8] S. Eckhardt, P.S. Brunetto, J. Gagnon, M. Priebe, B. Giese, K.M. Fromm, Chem. Rev. 113 (2013) 4708–4754.
[9] V.T. Yilmaz, C. Icsel, J. Batur, S. Aydinlik, P. Sahinturk, M. Aygun, Eur. J. Med. Chem. 139 (2017) 901–916.
[10] J. Jimenez, I. Chakraborty, M. Rojas-Andrade, P.K. Mascharak, J. Inorg. Biochem. 168 (2017) 13–17.
[11] C. O'Beirne, H.T. Althani, O. Dada, J. Cassidy, K. Kavanagh, H. Müller-Bunz, Y. Ortin, X. Zhu, M. Tacke, Polyhedron 149 (2018) 95–103.
[12] D. Armstrong, S.M. Kirk, C. Murphy, A. Guerriero, M. Peruzzini, L. Gonsalvi, A.D. Phillips, Inorg. Chem. 57 (2018) 6309–6323.
[13] G.J. Zhao, S.E. Stevens, Biometals 11 (1998) 7–32.
[14] G. Hogarth, Mini-Rev. Med. Chem. 12 (2012) 1202–1215.
[15] P. Ferreira, G.M. de Lima, E.B. Paniago, J.A. Takahashi, C.B. Pinheiro, Inorg. Chim. Acta 423 (2014) 443–449.
[16] A.C. Ekennia, D.C. Onwudiwe, A.A. Osowole, J. Sulfur Chem. 36 (2015) 96–104.
[17] S.K. Verma, V.K. Singh, J. Organomet. Chem. 791 (2015) 214–224.
[18] A.O. Ariza-Roldan, E.M. Lopez-Cardoso, M.E. Rosas-Valdez, P.P. Roman-Bravo, D.G. Vargas-Pineda, R. Cea-Olivares, M. Acevedo-Quiroz, R.S. Razo-Hernandez, P. Alvarez-Fitz, V. Jancik, Polyhedron 134 (2017) 221–229.
[19] S. Beniwal, S. Chhimpa, D. Gaur, P.J. John, Y. Singh, J. Sharma, Appl. Organomet. Chem. 31 (2017) e3725.
[20] S. Tamilvanan, G. Gurumoorthy, S. Thirumaran, S. Ciattini, Polyhedron 121 (2017) 70–79.
[21] J.O. Adeyemi, D.C. Onwudiwe, A.C. Ekennia, R.C. Uwaoma, E.C. Hosten, Inorg. Chim. Acta 477 (2018) 148–159.
[22] N.S. Jamaludin, S.N.A. Halim, C.-H. Khoo, B.-J. Chen, T.-H. See, J.-H. Sim, Y.-K. Cheah, H.-L. Seng, E.R.T. Tiekink, Z. Kristallogr. 231 (2016) 341–349.
[23] J.-H. Sim, N.S. Jamaludin, C.-H. Khoo, Y.-K. Cheah, S.N.A. Halim, H.-L. Seng, E.R.T. Tiekink, Gold Bull. 47 (2014) 225–236.
[24] B.-J. Chen, N.S. Jamaludin, C.-H. Khoo, T.-H. See, J.-H. Sim, Y.-K. Cheah, S.N.A. Halim, H.-L. Seng, E.R.T. Tiekink, J. Inorg. Biochem. 163 (2016) 68–80.
[25] Y.S. Tan, K.K. Ooi, K.P. Ang, A.M. Akim, Y.-K. Cheah, S.N.A. Halim, H.-L. Seng, E.R.T. Tiekink, J. Inorg. Biochem. 150 (2015) 48–62.
[26] Rigaku Oxford Diffraction. CrysAlis PRO, (2017).
[27] G.M. Sheldrick, Acta Crystallogr. A 64 (2008) 112–122.
[28] G.M. Sheldrick, Acta Crystallogr. C 71 (2015) 3–8.
[29] L.J. Farrugia, J. Appl. Crystallogr. 45 (2012) 849–854.
[30] DIAMOND, Visual Crystal Structure Information System, Version 3.1, CRYSTAL IMPACT, Postfach 1251, D-53002 Bonn, Germany, 2006.
[31] A.L. Spek, Acta Crystallogr. Sect. D 65 (2009) 148–155.
[32] J.H. Nelson, Concepts Magn. Reson. 14 (2002) 19–78.
[33] M.K. Milčič, V.B. Medaković, D.N. Sredojević, N.O. Juranić, S.D. Zarić, Inorg. Chem. 45 (2006) 4755–4763.
[34] E.R.T. Tiekink, J. Zukerman-Schpector, Chem. Commun. 47 (2011) 6623–6625.
[35] E.R.T. Tiekink, Coord. Chem. Rev. 345 (2017) 209–228.
[36] C.R. Groom, I.J. Bruno, M.P. Lightfoot, S.C. Ward, Acta Crystallogr. B 72 (2016) 171–179.
[37] A. Cingolani, Effendy, D. Martini, C. Pettinari, B.W. Skelton, A.H. White, Inorg. Chim. Acta 359 (2006) 2183–2193.
[38] C. Di Nicola, J. Ngoune, Effendy, C. Pettinari, B.W. Skelton, A.H. White, Inorg. Chim. Acta 360 (2007) 2935–2943.
[39] V. Kumar, V. Singh, A.N. Gupta, K.K. Manar, L.B. Prasad, M.G.B. Drew, N. Singh, New J. Chem. 38 (2014) 4478–4485.
[40] P.V.V.N. Kishore, J.-H. Liao, H.-N. Hou, Y.-R. Lin, C.W. Liu, Inorg. Chem. 55 (2016) 3663–3673.
[41] P. Nath, M.K. Bharty, B. Maiti, A. Bharti, R.J. Butcher, J.L. Wikaira, N.K. Singh, RSC Adv. 6 (2016) 93867–93880.
[42] M. Afzaal, C.L. Rosenberg, M.A. Malik, A.J.P. White, P. O'Brien, New J. Chem. 35 (2011) 2773–2780.
[43] Y.J. Tan, C.I. Yeo, N.R. Halcovitch, E.R.T. Tiekink, Z. Kristallogr. - New Cryst. Struct. 233 (2018) 513–515.
[44] D. Wallace, E.J. Quinn, D.R. Armstrong, J. Reglinski, M.D. Spicer, W.E. Smith, Inorg. Chem. 49 (2010) 1420–1427.
[45] T. Fiedler, T. Köller, B. Kreikemeyer, Front. Cell. Infect. Microbiol. 5 (2015) 15(11 pages).
[46] E. Freinkman, S. Chng, D. Kahne, Proc. Natl. Acad. Sci. U. S. A. 108 (2011) 2486–2491.
[47] M.V. Angelusiu, S. Barbuceanu, C. Draghici, G.L. Almajan, Eur. J. Med. Chem. 45 (2010) 2055–2062.
[48] M. Khandani, T. Sedaghat, N. Erfani, M.R. Haghshenas, H.R. Khavasi, J. Mol. Struct. 1037 (2013) 136–143.
[49] T. Sedaghat, M. Yousefi, G. Bruno, H. Amiri Rudbari, H. Motamedi, V. Nobakht, Polyhedron 79 (2014) 88–96.
[50] G.M. de Lima, D.C. Menezes, C.A. Cavalcanti, J.A.F. dos Santos, I.P. Ferreira, E.B. Paniago, J.L. Wardell, S.M.S.V. Wardell, K. Krambrock, I.C. Mendes, H. Beraldo, J. Mol. Struct. 988 (2011) 1–8.
[51] S. Leekha, C.L. Terrell, R.S. Edson, Mayo Clin. Proc. 86 (2011) 156–167.
[52] M.S. Svetlov, N. Vázquez-Laslop, A.S. Mankin, Proc. Natl. Acad. Sci. 114 (2017) 13673–13678.
[53] M.E. Levison, Infect. Dis. Clin. N. Am. 18 (2004) 451–465.
[54] F. van Bambeke, M.-P. Mingeot-Leclercq, Y. Glupczynski, P.M. Tulkens, Infect. Dis. (2017) 1162–1180.
[55] J.E. Maddison, A.D.J. Watson, J. Elliott, J.E. Maddison, S.W. Page, D.B. Church (Eds.), Small Animal: Clinical Pharmacology, Saunders/Elsevier, Edinburgh, 2008, pp. 148–185.
[56] V.H. Tam, A.N. Schilling, M. Nikolaou, J. Antimicrob. Chemother. 55 (2005) 699–706.
[57] P.J. Petersen, C.H. Jones, P.A. Bradford, Diagn. Microbiol. Infect. Dis. 59 (2007) 347–349.
[58] C. Vidaillac, J. Parra-Ruiz, M.J. Rybak, Diagn. Microbiol. Infect. Dis. 71 (2011) 470–473.
[59] A. Belley, E. Neesham-Grenon, F.F. Arhin, G.A. McKay, T.R. Parr, G. Moeck, Antimicrob. Agents Chemother. 52 (2008) 3820–3822.
[60] A. Roda, A. Minutello, M.A. Angellotti, A. Fini, J. Lipid Res. (1990) 1433–1443.
[61] H. Nabipour, S. Ghammamy, A. Rahmani, Micro Nano Lett. (2011) 217–220.
[62] A. Rabinkov, T. Miron, L. Konstantinovski, M. Wilchek, D. Mirelman, L. Weiner, Biochim. Biophys. Acta 1379 (1998) 233–244.